J Musculoskelet Neuronal Interact 2014; 14(3):255-266

Original Article

Hylonome

Bone loss in a new rodent model combining spinal cord injury and cast immobilization

J.F. Yarrow[1,3], F. Ye[1,3], A. Balaez[1], J.M. Mantione[1], D.M. Otzel[2], C. Chen[4], L.A. Beggs[1,3], C. Baligand[5], J.E. Keener[1], W. Lim[6], R.S. Vohra[6], A. Batra[6], S.E. Borst[2,3], P.K. Bose[1,7,8], F.J. Thompson[1,7], K. Vandenborne[6]

[1]Research Service and [2]Geriatrics Research, Education, and Clinical Center (GRECC), Department of Veterans Affairs Medical Center, North Florida/South Georgia Veterans Health System, Gainesville, FL, United States, 32608; Departments of [3]Applied Physiology & Kinesiology, [4]Orthopaedics & Rehabilitation, [5]Physiology and Functional Genomics, [6]Physical Therapy, [7]Physiological Sciences, and [8]Neurology, University of Florida, Gainesville, FL, United States, 32611

Abstract

Objectives: Characterize bone loss in our newly developed severe contusion spinal cord injury (SCI) plus hindlimb immobilization (IMM) model and determine the influence of muscle contractility on skeletal integrity after SCI. **Methods:** Female Sprague-Dawley rats were randomized to: (a) intact controls, (b) severe contusion SCI euthanized at Day 7 (SCI-7) or (c) Day 21 (SCI-21), (d) 14 days IMM-alone, (e) SCI+IMM, or (f) SCI+IMM plus 14 days body weight supported treadmill exercise (SCI+IMM+TM). **Results:** SCI-7 and SCI-21 exhibited a >20% reduction in cancellous volumetric bone mineral density (vBMD) in the hindlimbs ($p \leq 0.01$), characterized by reductions in cancellous bone volume (cBV/TV%), trabecular number (Tb.N), and trabecular thickness. IMM-alone induced no observable bone loss. SCI+IMM exacerbated cancellous vBMD deficits with values being >45% below Controls ($p \leq 0.01$) resulting from reduced cBV/TV% and Tb.N. SCI+IMM also produced the greatest cortical bone loss with distal femoral cortical area and cortical thickness being 14-28% below Controls ($p \leq 0.01$) and bone strength being 37% below Controls ($p \leq 0.01$). SCI+IMM+TM partially alleviated bone deficits, but values remained below Controls. **Conclusions:** Residual and/or facilitated muscle contractility ameliorate bone decrements after severe SCI. Our novel SCI+IMM model represents a clinically-relevant means of assessing strategies to prevent SCI-induced skeletal deficits.

Keywords: Spinal Cord Injury, Osteoporosis, Disuse, Fracture, micro CT

Introduction

Individuals who experience a functionally-complete spinal cord injury (SCI) exhibit severe lower extremity bone deficits that are thought to primarily result from the loss of motor function and load bearing activity below the lesion level[1]. This bone loss is characterized by rapid cancellous bone loss that occurs throughout the first several months to several years after SCI and more gradual cortical bone loss that continues for nearly a decade following injury, before reaching new steady state values[2]. This bone loss combines to produce a 20- to 100-fold greater bone fracture risk in those with SCI when compared with non-neurologically impaired age-matched individuals[3]. Fractures are both more common[4] and more severe in the SCI population, with the median length of inpatient hospitalization after bone fracture being 35 days[5]. As such, determining effective therapeutic strategies that prevent bone loss following SCI is of critical importance to the maintenance of musculoskeletal health within this population.

Numerous preclinical and clinical strategies have been evaluated as a means of restoring lower extremity musculoskeletal integrity following SCI. However, effective therapies to regenerate bone following SCI remain elusive, with bisphosphonate therapy[6] and mechanical overload[7] (i.e., the frontline pharmacologic and non-pharmacologic therapies for osteoporosis) providing only mild attenuation of bone loss following SCI and no

The authors have no conflict of interest.

Corresponding author: Joshua F. Yarrow, Ph.D., VA Medical Center, Research – 151, 1601 SW Archer Rd., Gainesville FL 32608-1197, United States
E-mail: jfyarrow@ufl.edu

Edited by: S. Warden
Accepted 23 June 2014

ability to regenerate bone. Additionally, at least one case-report evaluating functional electric stimulation of the quadriceps (a therapy capable of restoring muscle mass after SCI) has reported femoral fracture during treatment[8], indicating that severe bone loss represents an impediment to physical rehabilitation interventions intended to prevent muscle and bone loss after SCI.

An essential step in pursuing interventions to limit bone loss after SCI is the development of clinically-relevant models of SCI-induced bone loss. In this regard, the rat represents a well-established model that mimics both the site-specific bone loss occurring clinically after disuse and the loading-induced restoration of bone that occurs in humans[9]; albeit in a much shorter time frame because bone turnover is more rapid in rats than in humans[10]. The most severe rodent SCI bone loss model involves spinal cord transection[11] which does not mimic the histopathologic features of the majority of human SCIs that occur primarily from an initial blow to the spinal cord followed by spinal compression. Alternatively, the rodent mid-thoracic contusion SCI model closely reproduces the histopathologic features observed in the spinal cord and muscles following traumatic SCI in humans[12,13] and has been used to assess therapeutic strategies focused on alleviating musculoskeletal deficits following SCI[14,15]. Unfortunately, unlike humans, rodents exhibit residual muscle contractility and spontaneous recovery of hindlimb motor function and muscle mass after contusion SCI[15]. This functional recovery limits the ability of existing rodent contusion SCI models to mimic the more severe musculoskeletal deficits occurring clinically after *functionally-complete* SCI because even minimal walking ability after SCI maintains near-normal bone[16].

The primary purpose of this study was to evaluate bone loss in our newly developed rodent model that completely prevents sublesional loading via hindlimb cast immobilization (IMM) subsequent to severe contusion SCI[17]. Secondary purposes were to: 1) better characterize the time frame of bone loss after SCI, 2) determine the effects of residual muscle contractility on skeletal integrity after SCI, and 3) determine whether treadmill exercise represents a means of improving skeletal integrity after SCI+IMM. We hypothesized that SCI+IMM would exacerbate bone loss in comparison to SCI-alone and that assisted treadmill exercise would prevent bone loss in SCI+IMM animals.

Materials and methods

Animal care

16 week old (skeletally-mature) virgin female Sprague Dawley rats (body mass ranges from 280-300 g before SCI) were obtained from Charles River Laboratories (Indianapolis, IN). Animals were housed individually in a temperature- (22±1°C), humidity- (50±10%), and light-controlled animal housing facility (12h light: 12h dark cycle). Rats consumed rodent chow and water *ad libitum* and were given access to high-protein transgenic dough (Bio-Serv, NJ, product #S3472, 21.2% protein, 3.83 kcal/g) placed in the bottom of the cage. All experimental procedures were performed according to protocols approved by the Institutional Animal Care and Use Committee at the University of Florida and in accordance with the United States Government Principle for the Utilization and Care of Vertebrae Animals.

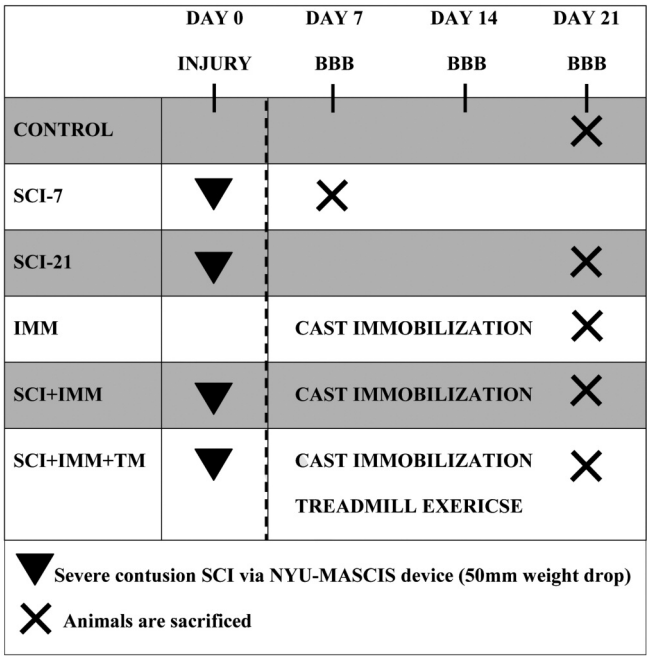

Figure 1. Experimental design. Contusion spinal cord injury (SCI) was performed on Day 0. Cast immobilization (IMM) and treadmill exercise (TM) were initiated at Day 7. Exercise was performed 5 days per week (20 minutes, twice daily) for 2 weeks. Animals were sacrificed at Day 21, with the exception of the SCI-7 group (sacrificed Day 7).

Experimental design

We acquired a subset of bones from a larger experiment that evaluated hindlimb muscle morphology and muscle force in a new rodent atrophy model combining severe contusion SCI+IMM[17]. Figure 1 depicts the timeline for all experiments from this study. Bones were acquired from the following groups: (a) intact controls (CTR, n=6), (b) severe contusion SCI sacrificed at day 7 (SCI-7, n=5), (c) severe contusion SCI sacrificed at day 21 (SCI-21, n=8), (d) intact animals undergoing bilateral hindlimb cast immobilization for two weeks (IMM, n=9), (e) severe contusion SCI plus IMM (SCI+IMM, n = 6), and (f) SCI+IMM plus partial body weight supported quadrupedal treadmill exercise for two weeks (SCI+IMM+TM, n=11). These groups were chosen because they exhibited the greatest muscle loss in our companion paper[17] and because we have previously demonstrated that TM exercise restores hindlimb muscle mass and improves locomotor function after moderate contusion SCI[15,18,19].

Surgery and post-operative care

An in-depth description of the aseptic surgical procedure has been previously reported[17]. Briefly, animals were anaes-

thetized with a combination of ketamine (90 mg/kg body weight) and xylazine (8 mg/kg body weight) and a laminectomy was performed at the thoracic vertebrae level T7-T9 to expose the spinal cord. Severe contusion SCI was produced using the NYU-MASCIS injury device and involved dropping a 10 g cylinder from the height of 50 mm onto the T8/T9 segment of the spinal cord and leaving the impactor on the spinal cord for 7 seconds thereafter. The average computer recorded force/velocity data from each drop were not different among groups (height: 49.60±0.11 mm, velocity: -0.95±0.01 m/sec, compression: 2.50±0.06 mm), indicating the injury was reproducible across the experiment.

Animals were provided subcutaneous lactated Ringers and ampicillin (200 mg/kg) post-surgery. Buprenorphine (0.025 mg/kg) and ketoprofen (22 mg/kg) were administered once daily for 48 hours. Postoperative care of the animals included daily examination for signs of distress, weight loss, dehydration, and bladder dysfunction. Manual expression of bladders was performed 2-3 times daily. Open-field locomotion was assessed by two blinded observers using the Basso-Beattie-Bresnahan (BBB) locomotor rating scale at weekly intervals[12]. Locomotor scores were <2.0 at post-injury week 1, <3.0 at week 2, and <5.0 at week 3, representing the presence of slight voluntary movement of 1-3 hindlimb joints (per leg) without voluntary hindlimb weight support and demonstrating the initiation of spontaneous hindlimb motor recovery.

Bilateral hind limb cast immobilization procedures

Bilateral hindlimb cast immobilization was performed according to our previous methods[17]. On Day 7, rats in the IMM, SCI+IMM, and SCI+IMM+TM groups were anaesthetized with isoflurane and fiberglass casting tape (Patterson Medical, Bolingbrook, IL, USA) was applied to both hindlimbs encompassing the caudal fourth of the body, with the exception of the abdomen (to allow access for bladder expression). Joints were fixed at the following angles: ankle=125°, knee=180°, and hip=160° with slight abduction. A soft thin padding layer was applied underneath the cast to prevent skin abrasions and the cast was adjusted or replaced 24 hours after initial application (if necessary) to ensure an appropriate tightness of the cast. Rats remained anesthetized during all casting procedures to ensure that no hindlimb loading occurred and were examined twice daily for skin lesions, hygiene, and fecal clearance.

Exercise training

Rodents in the SCI+IMM+TM underwent partial body weight supported, assisted quadrupedal TM training using a modified version of our previous protocol[18,20,21]. Beginning on Day 7, animals were given 5 minutes to explore the treadmill and then encouraged to walk on the moving treadmill (11 m/min). Subsequently, animals performed 20 minutes of partial body weight supported, assisted quadrupedal TM stepping twice daily (separated by a minimum of 2 hours), five days per week for two weeks. Two trainers conducted all TM training in order to standardize the protocol. Body weight support was provided by a harness connected to a counterweight offering 50% of body weight support during TM training to ensure the hindlimbs did not collapse during locomotion. Gait assistance was provided by placing the hind paws in plantar stepping throughout training because rats were incapable of voluntary stepping. Following training, the cast was immediately re-applied to the hindlimbs, which remained casted at all times except when undergoing training. In contrast, SCI+IMM animals remained casted throughout the intervention.

Tissue harvesting

Animals were euthanized at post-surgery Day 7 (SCI-7) or Day 21 (all other groups). The right and left femurs and tibias were removed, cleaned of surrounding soft tissue, weighed, and lengths measured. The femurs were wrapped in salinated gauze and stored at -20°C to maintain bone mechanical characteristics[22] and the tibias were stored at -80°C for further analysis.

μCT evaluation of bone mineral density and cancellous morphometry

The right distal femoral metaphysis, proximal tibial metaphysis, and femoral neck were thawed to room temperature and scanned with a Bruker Skyscan 1172 μCT (Kontich, Belgium) at 80 kVP/120 μA with a 0.5 mm aluminum filter, 1 k camera resolution, 19.2 μm voxel size, 0.5° rotation step, and 180° tomographic rotation. The cancellous region of interest (ROI) at the femoral metaphysis began 1.5 mm proximal to the growth plate and encompassed a total of 4 mm. The cortical ROI at the femoral metaphysis began 3 mm proximal to the growth plate (in order to completely avoid residual growth plate) and encompassed a total of 2.5 mm. The tibial metaphysis ROI began 2.5 mm distal to the growth plate and encompassed a total of 2.5 mm. The femoral neck ROI encompassed 0.35 mm surrounding the smallest diameter of the neck. Reliable μCT analysis of cortical bone could not be performed at the proximal tibia because *in situ* assessment of muscle mechanical force was performed in our companion paper[17] which produces significant cortical (but not cancellous) bone abnormalities at this skeletal site.

Cross-sectional images were reconstructed using a filtered back-projection algorithm (NRecon, Kontich, Belgium). Three-dimensional (3D) medullary volumetric (v)BMD (cancellous bone only) was calculated using CTan software (version #1.13.1.1, Bruker Skyscan, Kontich, Belgium) within the previously defined ROIs and total/*integral* vBMD (cortical plus cancellous bone) was assessed at the femoral neck. Densities were determined following calibration with hydroxyapatite phantoms. 3D morphometric measurements were also determined at the distal femur (cancellous and cortical) and proximal tibia (cancellous only) ROIs and include: cancellous bone volume (cBV/TV, %), trabecular number (Tb.N, #/mm), trabecular separation (Tb.Sp, mm), trabecular thickness (Tb.Th, mm), structural model index (SMI), total cross-sectional area inside the periosteal envelope (Tt.Ar, mm^2), cortical bone area (Ct.Ar, mm^2), medullary area (Ma.Ar, mm^2), cortical area fraction (Ct.Ar/Tt.Ar, %), and average cortical thickness (Ct.Th, mm).

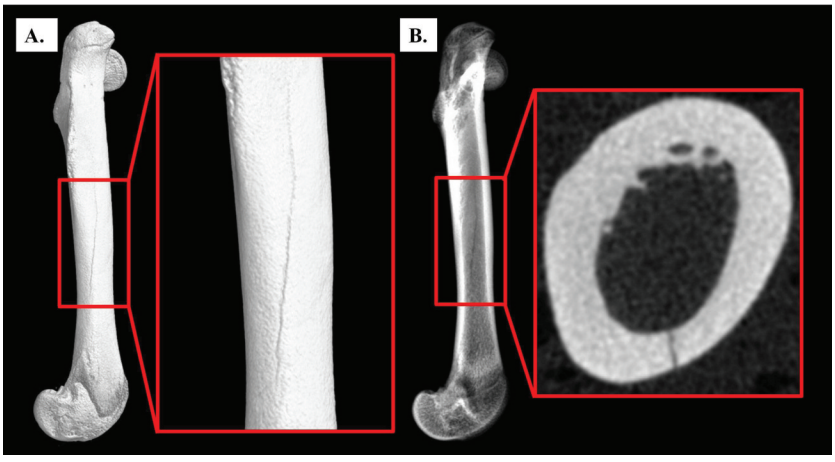

Figure 2A-B. Complete longitudinal fracture of the femoral shaft. Surface (A) and radiographic (B) images of a complete longitudinal fracture that extends from the femoral midshaft to the distal femur. Fractures were present in 8 animals from the SCI-21 (n=5), SCI+IMM (n=1), and SCI+IMM+TM (n=2) groups. Imaged via μCT with 19.1 μm voxel size.

	CTR (a)	SCI-7 (b)	SCI-21 (c)	IMM (d)	SCI+IMM (e)	SCI+IMM+TM (f)
TOTAL BODY						
Mass at sacrifice, g	325±7[c,d*,e*,f*]	295±8[d,f]	289±8[a]	267±5[a*,b]	272±6[a*]	266±6[a*,b]
FEMUR						
Length, mm	36.9±0.6[b]	35.0±0.3[a]	36.4±0.3	35.9±0.3	35.8±0.3	35.4±0.3
Mass, g	0.99±0.02[b*,e*,f*]	0.84±0.03[a*]	0.91±0.03	0.90±0.02	0.82±0.02[a*]	0.87±0.02[a*]
TIBIA						
Length, mm	40.9±0.2[b*,d,e]	38.8±0.3[a*,c*]	40.4±0.3[b*]	39.4±0.3[a]	39.4±0.3[a]	39.9±0.2
Mass, g	0.76±0.01[e]	0.67±0.02	0.72±0.03	0.69±0.02	0.66±0.02[a]	0.72±0.01[a,e]

Values are Means±SE of n=5-11/group. Letter a-f indicate differences from respectively labeled groups at p≤0.05 or *p≤0.01 (a= vs. CTR, b= vs. SCI-7, c= vs. SCI-21, d= vs. IMM, e= vs. SCI+IMM, f= vs. SCI+IMM+TM).

Table 1. Body mass and whole bone characteristics at sacrifice.

Evaluation of bone mechanical characteristics

Subsequent to μCT, the distal femoral metaphysis underwent a modified anterior-posterior compression and bending test[23] using a servohydraulic testing machine (MTS 858 Bionix Test System, MTX, Eden Prairie, MN). We performed mechanical testing of the distal femur because fractures occur commonly at this skeletal site in the clinical SCI population and result in extensive hospitalization[4,5]. Briefly, the femora were thawed to room temperature and remained wrapped in saline soaked gauze except during measurements. The proximal femur was embedded in Bondo fiberglass resin (3 M, St. Paul, MN) in a rectangular cuvette with only the distal 8mm of the femur exposed and the bone (cuvette) was placed horizontally. Prior to initiation of testing, 10 cycles of sinusoidal preload (from 0 to 10 N) were applied in the vertical direction to the anterior portion of the distal femoral metaphysis using a flat steel fixture. The compression load was subsequently applied at 1.0 mm/sec until failure of the specimen. Fracture occurred at the distal femur within the previously defined cortical/cancellous ROI. The maximum load, displacement at maximum load, and stiffness were determined from the load-deformation curves.

Statistical analysis

Results are reported as Means±SEM and an α level of p≤0.05 was defined as the threshold of significance. One-Way ANOVAs were used to separately analyze normally distributed data and the Tukey's posthoc test was performed for multiple comparisons among groups when appropriate. The non-parametric Kruskal-Wallis ANOVA and Mann-Whitney U tests were performed when data were not normally distributed. Pearson correlation coefficients were performed to as-

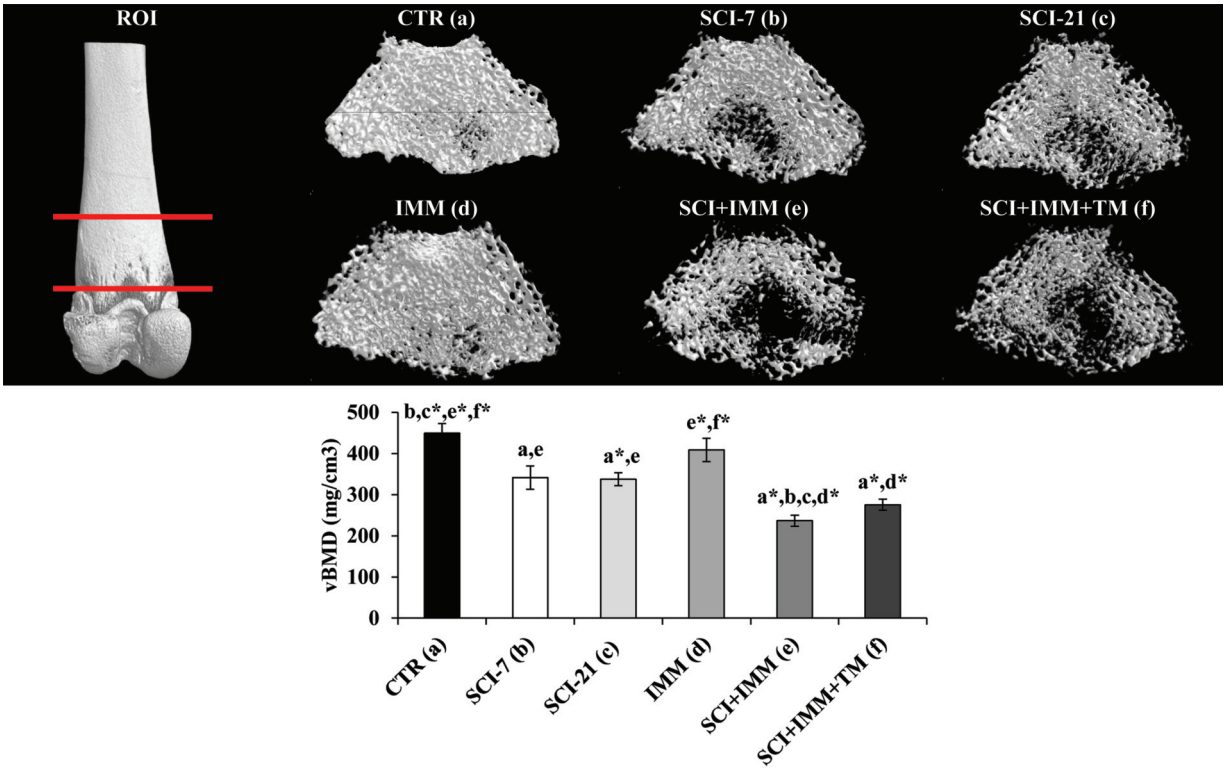

Figure 3. Cancellous volumetric bone mineral density (vBMD) at the distal femur measured via µCT. Images are 3D renditions of cancellous bone within the distal femoral metaphysis ROI, which began 1.5mm proximal to the growth plate and encompassed a total of 4mm. Values are Means±SE or n =5-11/group. Letters a-f indicate differences from respectively labeled groups at p≤0.05 or *p≤0.01 (a= vs. CTR, b= vs. SCI-7, c= vs. SCI-21, d= vs. IMM, e= vs. SCI+IMM, f= vs. SCI+IMM+TM).

sess associations between skeletal morphometric and bone mechanical characteristics. All statistical analyses were performed with the SPSS v15.0.0 statistical software package (Chicago, IL).

Results

Animal health and body/tissue characteristics

Animals displayed normal grooming behavior and no signs of stress after SCI or IMM, with no skin abrasions observed throughout the intervention. No differences in body mass were present among groups at baseline (data not shown). Body mass and whole bone characteristics at sacrifice are presented in Table 1. SCI induced an expected reduction in body mass that was relatively consistent among all treatment groups. Femur and tibia length/mass were also consistent across treatment groups. Unexpectedly, we observed (via µCT imaging) the presence of complete non-remodeled longitudinal fractures initiating approximately 11mm from the distal end of the femur and extending proximally at least one-third the length of the femur in a small subset of animals from the SCI-21 (n=5), SCI+IMM (n=1), and SCI+IMM+TM (n=2) groups (Figure 2A-B); the etiology of which remains unknown. Fracture presence did not appear to interfere with µCT analysis of bone morphology nor bone mechanical testing (at the femoral metaphysis) because fractures were completely encased in the fiberglass resin during testing. Subsequent statistical analyses verified no differences in mechanical characteristics were present between fractured versus non-fractured bones within each group.

µCT analysis of volumetric bone mineral density

Cancellous (medullary) vBMD was 21-25% lower at the distal femur (Figure 3) and proximal tibia (Figure 4) in SCI-7 and SCI-21 animals compared with CTR (p≤0.01), with no differences among SCI groups. In intact animals, IMM-alone did not induce cancellous vBMD changes at either skeletal site. In SCI+IMM animals vBMD values were 45-47% lower than CTR (p≤0.01) and 25-30% lower than SCI-21 (p≤0.01), representing the lowest values of any group. Adjunctive TM exercise partially prevented the reduction in proximal tibia vBMD resulting from SCI+IMM, with vBMD values being 21% higher in SCI+IMM+TM versus SCI+IMM (p≤0.01). However, proximal tibia vBMD remained 33% below CTR (p≤0.01) and 15% below SCI-21 (p≤0.05) in SCI+IMM+TM animals. In contrast, distal femoral cancellous vBMD was not different among SCI+IMM and SCI+IMM+TM animals.

Femoral neck cancellous vBMD deficits were not present in SCI-7 or IMM groups; whereas, cancellous vBMD was 19-25% lower in SCI-21, SCI+IMM, and SCI+IMM+TM animals com-

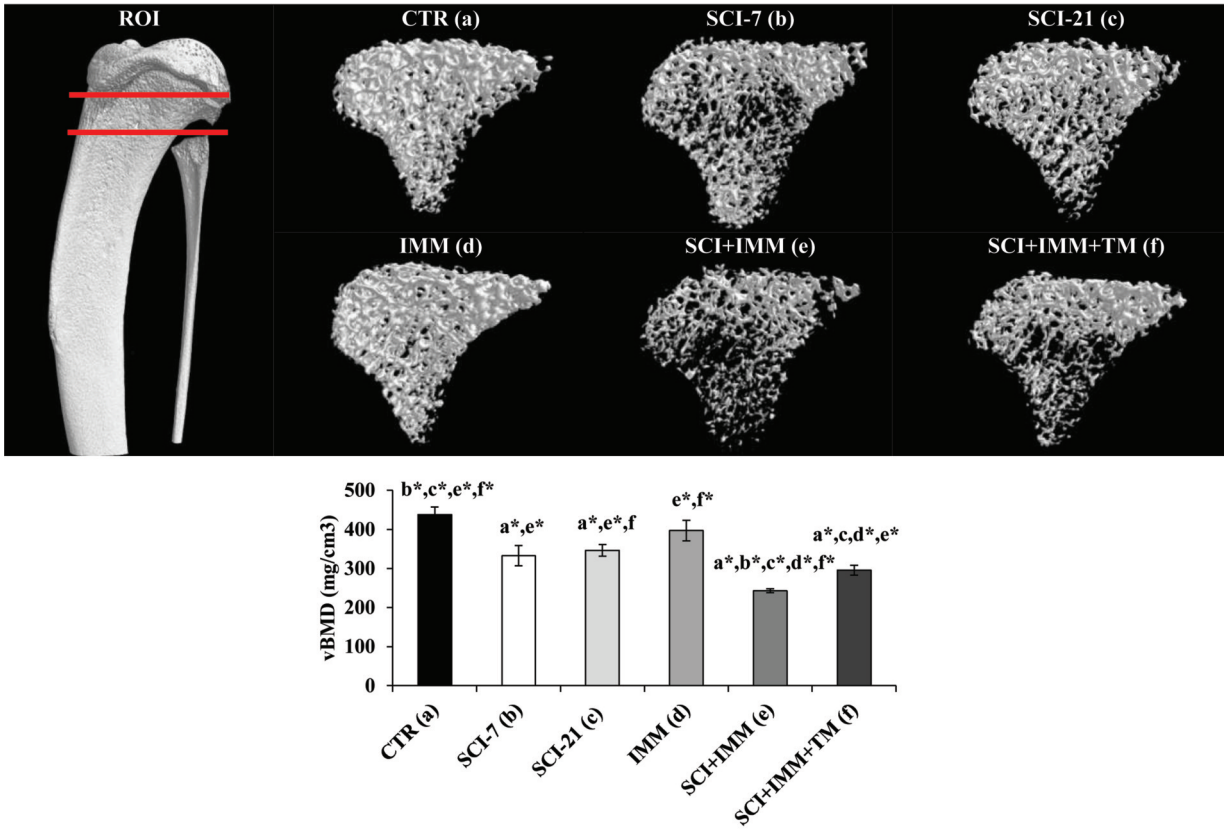

Figure 4. Cancellous volumetric bone mineral density (vBMD) at the proximal tibia measured via µCT. Images are 3D renditions of cancellous bone within the proximal tibial ROI which began 2.5mm distal to the growth plate and encompassed a total of 2.5mm. Values are Means±SE or n=5-11/group. Letters a-f indicate differences from respectively labeled groups at p≤0.05 or *p≤0.01 (a= vs. CTR, b= vs. SCI-7, c= vs. SCI-21, d= vs. IMM, e= vs. SCI+IMM, f= vs. SCI+IMM+TM).

pared with CTR (p≤0.01, Figure 5), with no differences among groups receiving SCI. No differences were present among groups for femoral neck total/integral vBMD (data not shown).

µCT analysis of cancellous bone morphometry and microarchitecture

Cancellous µCT outcomes from the distal femoral and proximal tibial metaphyses are presented in Table 2. cBV/TV% was 36-40% lower in SCI-7 (p≤0.05 femur and p≤0.01 tibia) and SCI-21 animals (p≤0.01 at both skeletal sites) compared with CTR. These differences were characterized by 25-36% lower Tb.N (p≤0.01), 10-21% lower Tb.Th (p≤0.01 for femur SCI-21 and non-significant for others), and a 16-50% increase in Tb.Sp (p≤0.01 for SCI-7 femur and p≤0.05 for SCI-7 tibia and SCI-21 tibia) when compared with CTR, with no differences present among SCI-7 and SCI-21 groups. IMM-alone did not induce cancellous morphometric deficits at either skeletal site. In contrast, SCI+IMM produced the greatest cancellous bone losses with cBV/TV% being 68-72% lower than CTR (p≤0.01) and 48-53% lower than SCI-21 animals (p≤0.01) at both skeletal sites. These deficits occurred via concomitant reductions in Tb.N and Tb.Th, with Tb.N being 55-58% lower than CTR (p≤0.01) and 40% lower than SCI-21 (p≤0.01) and Tb.Th being 28-40% lower than CTR (p≤0.01 femur and p≤0.05 tibia) and 11-18% lower than SCI-21 (non-significant). Tb.Sp was also 50-95% higher in SCI+IMM animals compared with CTR and SCI-21 animals (p≤0.01). Adjunctive treadmill exercise partially prevented the cancellous bone losses resulting from SCI+IMM, as evidenced by 45-52% higher cBV/TV% (p≤0.01 femur and p≤0.05 tibia), 36-37% higher Tb.N (p≤0.01 femur and p≤0.05 tibia), and 15-23% lower Tb.Sp (p≤0.01 femur and p≤0.05 tibia) in SCI+IMM+TM animals compared with SCI+IMM. However, cBV/TV% remained 54-57% lower at the distal femur and proximal tibia of SCI+IMM+TM animals versus CTR (p≤0.01) and 22-25% lower compared to SCI-21 (p≤0.05), with Tb.N being 38-43% below CTR (p≤0.01) and 18-19% below SCI-21 (p≤0.05 for femur and non-significant for tibia) and Tb.Sp being 47-50% higher than CTR (p≤0.01) and 27% higher than SCI-21 animals (p≤0.01) at both skeletal sites.

Structural model index (SMI), a measure of the geometric characteristics of individual trabeculae (Table 2), was elevated to a roughly similar magnitude in SCI-7 animals (p≤0.05 femur and p≤0.01 tibia) and SCI-21 animals (p≤0.01 at both

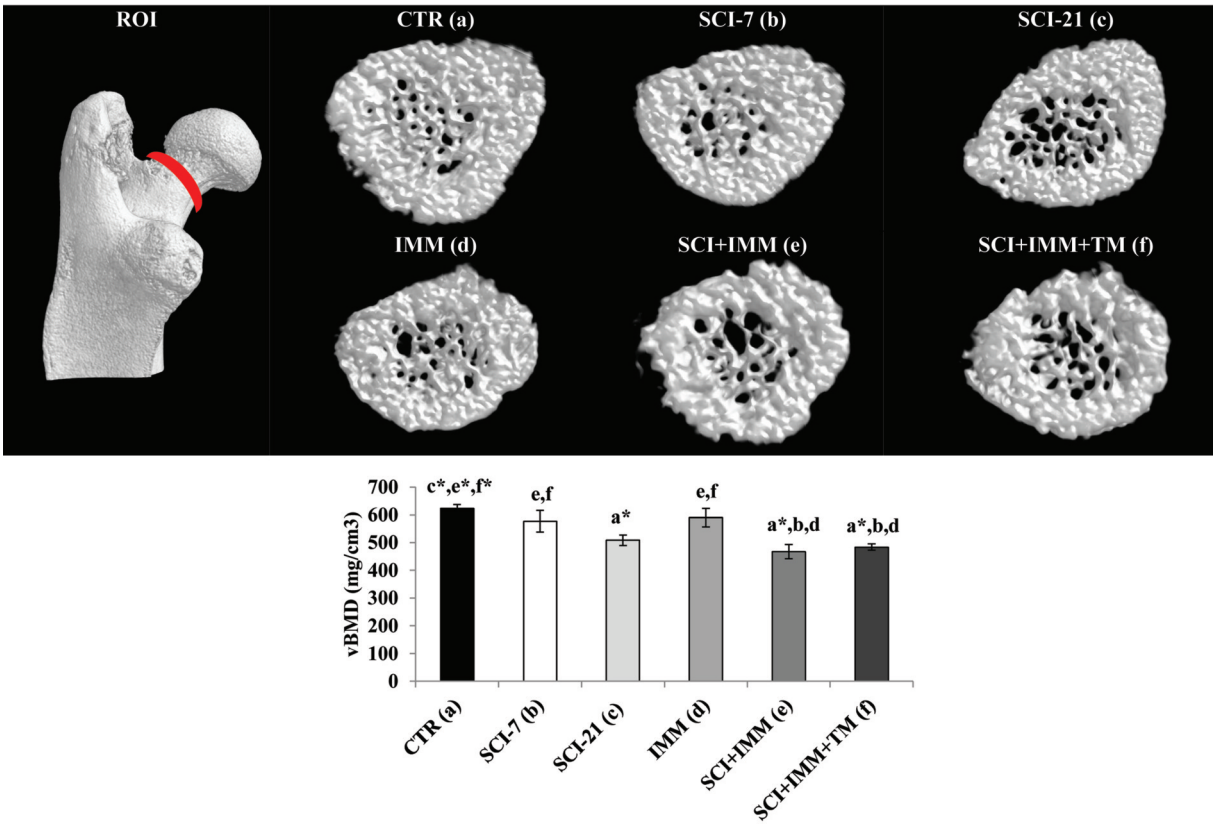

Figure 5. Cancellous volumetric bone mineral density (vBMD) at the femoral neck measured via µCT. Images are 3D renditions of cancellous bone within the femoral neck ROI, which encompassed 0.35 mm surrounding the smallest diameter of the neck. Values are Means±SE or n=5-11/group. Letters a-f indicate differences from respectively labeled groups at p≤0.05 or *p≤0.01 (a= vs. CTR, b= vs. SCI-7, c= vs. SCI-21, d= vs. IMM, e= vs. SCI+IMM, f= vs. SCI+IMM+TM).

	CTR (a)	SCI-7 (b)	SCI-21 (c)	IMM (d)	SCI+IMM (e)	SCI+IMM+TM (f)
DISTAL FEMUR						
BV/TV, %	44.0±3.2^{b,c*,e*,f*}	28.0±3.8^{a,e*,f}	26.4±2.2^{a*,e*,f}	37.7±4.0^{e*,f*}	12.5±0.2^{a*,b*,c*,d*,f*}	19.0±1.6^{a*,b,c,d*,e*}
Tb.N, #/mm	3.00±0.11^{b*,c*,e*,f*}	2.30±0.20^{a*,e*}	2.30±0.12^{a*,e*,f}	2.66±0.16^{e*,f*}	1.36±0.05^{a*,b*,c*,d*,f*}	1.86±0.10^{a*,c,d*,e*}
Tb.Th, mm	0.15±0.01^{c*,e*,f*}	0.12±0.01^{e}	0.11±0.00^{a*,d}	0.14±0.01^{c,e*,f*}	0.09±0.00^{a*,b,d*}	0.10±0.00^{a*,d*}
Tb.Sp, mm	0.22±0.01^{b*,e*,f*}	0.33±0.04^{a*}	0.26±0.02^{e*,f*}	0.25±0.02^{e*,f*}	0.43±0.02^{a*,c*,d*,f*}	0.33±0.01^{a*,c*d*,e*}
SMI	0.55±0.24^{b,c*,e*,f*}	1.56±0.18^{a,e}	1.82±0.10^{a*,d}	0.99±0.28^{c,e*,f*}	2.45±0.04^{a*,b,d*}	2.13±0.09^{a*,d*}
PROXIMAL TIBIA						
BV/TV, %	32.6±2.3^{b*,c*e*,f*}	19.9±3.2^{a*,e*}	20.1±1.7^{a*,e*,f}	28.9±3.2^{e*,f*}	10.4±0.7^{a*,b*,c*,d*,f}	15.1±1.3^{a*,c,d*,e}
Tb.N, #/mm	3.05±0.12^{b*,c*,e*,f*}	1.96±0.29^{a*}	2.14±0.17^{a*e*}	2.66±0.19^{e*,f*}	1.29±0.07^{a*,c*,d*,f}	1.75±0.13^{a*,d*,e}
Tb.Th, mm	0.11±0.00^{e}	0.10±0.01	0.09±0.00	0.11±0.00^{e*}	0.08±0.00^{a,d*}	0.09±0.01
Tb.Sp, mm	0.19±0.01^{b,c,e*,f*}	0.27±0.02^{a}	0.22±0.01^{a,e*,f*}	0.22±0.01^{e*,f*}	0.33±0.01^{a*,c*,d*,f}	0.28±0.01^{a*,c*,d*,e}
SMI	1.57±0.13^{b*,c*,e*,f*}	2.34±0.18^{a*}	2.28±0.07^{a*}	1.92±0.13^{e*,f*}	2.63±0.05^{a*,d*}	2.53±0.08^{a*,d*}

Values are Means±SE of n=5-11/group. Letter a-f indicate differences from respectively labeled groups at p≤0.05 or *p≤0.01 (a= vs. CTR, b= vs. SCI-7, c= vs. SCI-21, d= vs. IMM, e= vs. SCI+IMM, f= vs. SCI+IMM+TM).

Table 2. Cancellous structural characteristics at the distal femoral and proximal tibial metaphyses measured via µCT.

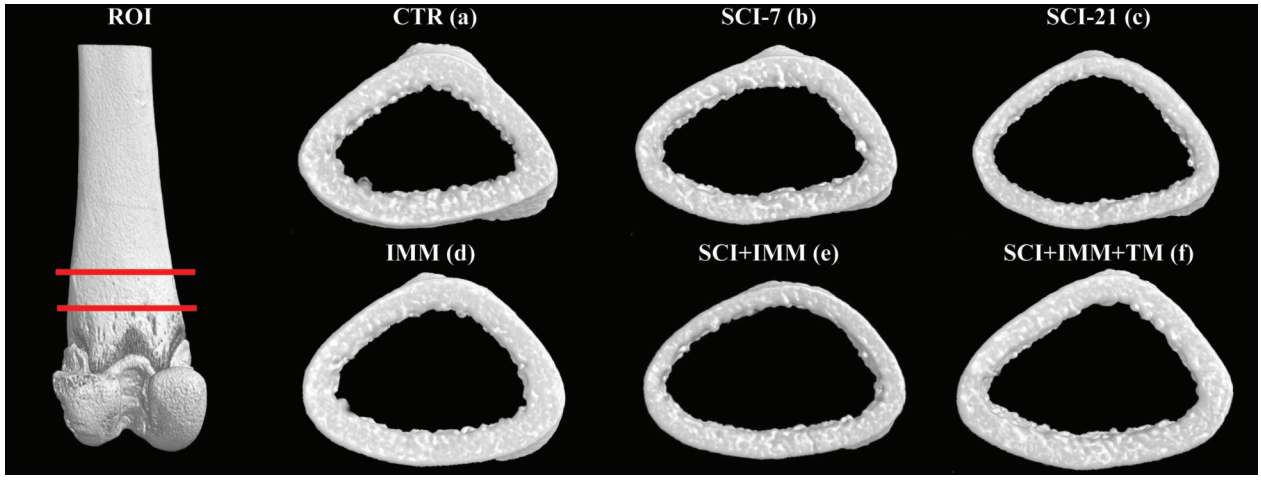

Figure 6. Representative 3D renditions of cortical bone at the distal femur acquired via µCT. The cortical ROI began 3mm proximal to the growth plate (in order to completely avoid residual growth plate) and encompassed a total of 2.5mm. Note visibly reduced cortical thickness (Ct.Th) and cortical area (Ct.Ar) in SCI-21 and SCI+IMM bones. Adjunctive TM exercise partially alleviated cortical bone loss. Actual values are presented in Table 3.

	CTR (a)	SCI-7 (b)	SCI-21 (c)	IMM (d)	SCI+IMM (e)	SCI+IMM+TM (f)
Tt.Ar, mm^2	14.3±0.5^{e}	13.4±0.6	13.7±0.7	13.6±0.4	11.8±0.5^{a}	13.2±0.3
Ct.Ar, mm^2	6.38±0.16^{c*,e*,f*}	5.67±0.16^{e*}	5.11±0.12^{a*,d*}	5.88±0.16^{c*,e*}	4.59±0.14^{a*,b*,d*,f*}	5.39±0.14^{a*,e*}
Ma.Ar, mm^2	7.95±0.40	7.78±0.50	8.57±0.71	7.74±0.34	7.22±0.43	7.67±0.22
Ct.Ar/Tt.Ar, %	44.7±1.0	42.3±1.1	38.1±2.3	43.4±1.3	39.1±1.7	41.9±1.0
Ct.Th, mm	0.49±0.01^{c,e*}	0.47±0.01	0.43±0.01^{a,d}	0.48±0.01^{c,e}	0.42±0.02^{a*,d}	0.47±0.01

Values are Means±SE of n=5-11/group. Letter a-f indicate differences from respectively labeled groups at p≤0.05 or *p≤0.01 (a= vs. CTR, b= vs. SCI-7, c= vs. SCI-21, d= vs. IMM, e= vs. SCI+IMM, f= vs. SCI+IMM+TM).

Table 3. Cortical structural characteristics at the distal femur measured via µCT.

skeletal sites) compared to CTR. IMM-alone did not alter SMI at either skeletal site. In contrast, SMI was highest in SCI+IMM animals, with values being higher than CTR (p≤0.01) at both skeletal sites. SCI+IMM+TM did not prevent this increase, with values remaining higher than CTR (p≤0.01).

µCT analysis of cortical bone morphometry

Representative three-dimensional renditions of the cortical bone at the distal femur are illustrated in Figure 6 and cortical µCT outcomes from this skeletal site are presented in Table 3. Neither SCI-7 nor IMM-alone induced cortical bone deficits at this skeletal site. In SCI-21 animals, Ct.Ar and Ct.Th were 20% (p≤0.01) and 12% (p≤0.05) lower than CTR, respectively. SCI+IMM induced the greatest cortical deficits at this skeletal site with Tt.Ar being 17% lower than CTR (p≤0.05), resulting from a 28% lower Ct.Ar (p≤0.01) and 14% lower Ct.Th (p≤0.01) compared with CTR. Adjunctive TM exercise partially prevented the cortical bone deficits resulting from SCI+IMM, as evidenced by 17% higher Ct.Ar (p≤0.01) in SCI+IMM+TM animals compared with SCI+IMM. However, Ct.Ar remained 16% lower than CTR in SCI+IMM+TM animals (p≤0.01).

Bone mechanical testing

The distal femoral mechanical characteristics are presented in Table 4. Neither SCI-7 nor IMM-alone induced alterations in maximum load at this skeletal site. In SCI-21 animals, distal femoral bone strength was 21% lower than CTR (p≤0.05). SCI+IMM produced the greatest deficit in bone strength, with values being 37% lower than CTR (p≤0.01). Adjunctive TM exercise did not prevent bone strength deficits with values in SCI+IMM+TM animals remaining 26% below CTR (p≤0.05). Displacement at maximum load was not different among groups. No differences in bone stiffness were present between

	CTR (a)	SCI-7 (b)	SCI-21 (c)	IMM (d)	SCI+IMM (e)	SCI+IMM+TM (f)
DISTAL FEMUR						
Maximum Load, N	95±4[c,e*,f]	84±4[d*]	75±4[a,d*]	115±8[b*,c*,e*,f*]	59±9[a*,d*]	70±5[a,d*]
Displacement, mm	0.90±0.06	1.16±0.08	0.83±0.07	0.99±0.15	1.04±0.20	0.87±0.09
Stiffness, N/mm	136±17[e]	82±8[d*]	99±8[d]	159±23[b*,c,e*,f*]	65±10[a,d*]	87±7[d*]

Values are Means±SE of n=5-11/group. Letter a-f indicate differences from respectively labeled groups at p≤0.05 or *p≤0.01 (a= vs. CTR, b= vs. SCI-7, c= vs. SCI-21, d= vs. IMM, e= vs. SCI+IMM, f= vs. SCI+IMM+TM).

Table 4. Mechanical characteristics of the distal femur.

CTR, SCI-7, or SCI-21 animals. Stiffness was lower in SCI+IMM when compared with CTR (p≤0.05) and IMM animals (p≤0.01). Adjunctive TM exercise appeared to increase stiffness in comparison with SCI+IMM, but group differences did not reach significance.

Discussion

The severe bone loss[2] and high fracture risk occurring after SCI[3-5] represent impediments to physical rehabilitation strategies intended to restore musculoskeletal integrity in this population. An essential step in identifying effective therapies to restore bone subsequent to SCI is the development of improved models of contusion SCI-induced bone loss and the evaluation of the characteristics that underlie musculoskeletal integrity after injury. Herein, we characterize cancellous and cortical bone loss in a newly developed rodent model that combines severe mid-thoracic contusion SCI with hindlimb IMM[17]. The primary finding of this study is that IMM exacerbates bone loss subsequent to severe contusion SCI, demonstrating the biologic role and clinical importance of residual muscle contractility on bone maintenance after SCI. We also evaluated the time frame in which bone loss occurs subsequent to SCI and observed that the vast majority of cancellous bone loss occurred within the first 7 days of injury in rodents, while cortical bone loss was delayed. Additionally, we demonstrated that two-weeks of partial body weight supported TM exercise represents a means of mitigating cancellous and cortical bone loss in this model. These results suggest that mechanisms other than disuse may influence bone loss in the early time periods after SCI, especially given that 14 days of IMM induced no observable bone deficits in intact animals.

Several rodent models of SCI-induced bone loss exist in the literature[11,16,24]. Spinal cord transection typically results in more severe bone loss[11] than contusion SCI[16]. However, the rodent mid-thoracic contusion SCI model more closely reproduces the histopathologic features of the most common form of traumatic SCI in humans[12,13], illustrating our rationale for selecting this model and the clinical relevance of this type of injury. In this regard, we evaluated the effects of severe contusion SCI on bone loss at several common fracture sites that exist within the clinical SCI population[4,5], including the distal femur, proximal tibia, and femoral neck of skeletally-mature rats. Robust cancellous and cortical bone loss was observed at each site within 21 days of injury. In general, cancellous bone deficits were characteristically similar and of an equal magnitude at the distal femur and proximal tibia; whereas, slightly less cancellous bone loss occurred at the femoral neck. Evaluation of cancellous bone at the distal femur provided a more consistent analysis than at the proximal tibia, similar to what has been reported clinically[25]. Importantly, the skeletal adaptations that occur within 7-21 days in the adult rat mimic changes occurring over several months to approximately two years in adult humans[26], which is the time frame when the greatest reductions in cancellous bone loss occurs clinically after SCI[27,28]. This apparent temporal disconnect occurs because bone turnover rates are more rapid in rats than humans[10]. However, unlike humans, rodents exhibit spontaneous recovery of hindlimb motor function after contusion SCI[16], which partially protects against the muscle deficits occurring after injury[15]. In order to determine if this was also the case for bone deficits and to overcome this potential limitation, we evaluated the skeletal effects of IMM-alone and SCI+IMM. Bone deficits were not observed in uninjured animals after 14 days of IMM-alone in our experiment. In contrast, SCI+IMM exacerbated cancellous bone loss at all skeletal sites, primarily via reduced Tb.N, and provided the greatest magnitude of cortical bone loss. Importantly, bone deficits in our newly developed SCI+IMM model were of a comparable magnitude to that reported following spinal cord transection[11] and much greater than that reported following other severe contusion SCI models over a similar time frame[16], likely because our newly developed SCI+IMM model limits the recovery of hindlimb muscle function[17] and completely eliminates hindlimb weight bearing subsequent to SCI. As such, both denervation (via SCI) and disuse appear to be primary factors driving the rapid skeletal deficits that occur in the early time periods after SCI.

To better characterize our model, we evaluated the time frame in which bone loss occurs after SCI. Surprisingly, cancellous bone deficits were identical at 7 days post-injury and 21 days post-injury, demonstrating that cancellous bone loss occurs quite rapidly following SCI in our model and subsequently stabilizes thereafter. This finding mimics that which has been observed clinically following complete SCI, in which

a lower BMD steady state is established subsequent to rapid bone loss occurring quickly after injury[29]. In contrast, cortical bone deficits were not observed until 21 days post-SCI, mimicking the delayed nature of cortical bone loss that is present clinically after SCI[2]. In this regard, the rapidity and severity of bone loss in our SCI+IMM model raises several unique possibilities. First, it appears that mechanisms other than disuse (e.g., denervation or hormonal irregularities) may underlie bone loss after SCI, as others have suggested[30], especially given that we did not observe bone deficits following 14 days of hindlimb IMM-alone in intact animals. Second, it appears that residual muscle contractility and/or the initiation of spontaneous muscle recovery (which typically begins 14 days after contusion SCI in rodents) may provide some protection against bone loss after SCI, similar to the effects observed in other disuse models[31]. In support of this contention, we have previously reported that SCI+IMM produces greater hindlimb muscle loss than either SCI- or IMM-alone[15], demonstrating that even a small amount of residual muscle contractility provides some musculoskeletal benefit after SCI. This argument is strengthened by the observation that body weight supported TM exercise partially prevented bone deficits resulting from SCI+IMM, indicating that only a small threshold of mechanical loading is necessary to ameliorate bone loss resulting from disuse. Regardless, bone volume following two weeks of TM exercise subsequent to SCI+IMM remained below CTR values and even that of SCI-alone (in the case of cancellous bone), which is not entirely surprising given that osteoblasts isolated from rats undergoing SCI respond less robustly to mechanical strain than osteoblasts from uninjured animals[32]. Similarly, physical rehabilitation strategies (e.g., partial body weight supported treadmill exercise or functional electrical stimulation) have shown only a modest ability to attenuate bone loss in humans with SCI[7] or in animal models of SCI[33], despite their apparent effectiveness in restoring muscle mass after SCI[1].

One unexpected finding we observed was the presence of complete longitudinal femoral fractures present in several animals receiving SCI, with no fractures present in the tibiae or in uninjured animals. We are unaware of any previous report of bone fracture in rodent SCI models. However, several case reports indicate that low-energy trauma may induce stress fractures in postmenopausal women that are characteristically similar to those we observed[34,35]. Humans with SCI exhibit a 20- to 100-fold greater fracture risk than able-bodied individuals[3] and at least one case-report exists describing femoral fracture resulting from functional electric stimulation of the quadriceps after SCI[8], underlying the importance of our unique observation. In this regard, we evaluated the shape (architecture) of trabeculae (reported as SMI) because trabecular architecture is highly predictive of maximal cancellous bone strength[36]. SMI values were elevated subsequent to SCI and were highest in SCI+IMM animals, representing increased rod-like trabecular structures and reduced plate-like trabecular structures[37] which indicates a structurally weaker trabecular architecture[36]. Additionally, we evaluated maximal bending strength at the distal femur and observed that bone strength was reduced by SCI and was lowest in SCI+IMM animals, likely because the quantity and quality of both cortical and cancellous bone were reduced by these treatments at this skeletal site. However, we cannot exclude the possibility that fractures occurred post-mortem because *in vivo* verification of fracture presence was not performed due to the unexpected nature of this finding. Regardless, both direct and indirect measurements indicate that bone strength was lowest in SCI+IMM animals.

In summary, we have developed a new rodent atrophy model that combines severe contusion SCI and IMM in order to limit the spontaneous recovery of hindlimb muscle contractility and eliminate hindlimb loading subsequent to SCI, which addresses an existing limitation of all current rodent contusion SCI models focused on musculoskeletal recovery. Cancellous and cortical bone loss was more severe in our SCI+IMM model than that occurring with contusion SCI-alone. Interestingly, the majority of SCI-induced cancellous bone deficits occurred in the first 7 days post injury and stabilized thereafter, while the cortical bone deficits were delayed. Body weight supported TM exercise partially ameliorated bone loss resulting from SCI+IMM, demonstrating that a relatively low threshold of mechanical loading alleviates bone loss after SCI. However, future studies evaluating histomorphometric or circulating markers of bone turnover are necessary to determine whether TM training exerts antiresorptive and/or osteoanabolic effects on bone after SCI. In conclusion, our newly developed SCI+IMM model exhibits many skeletal characteristics present in the clinical SCI population and use of this model appears to be an appropriate means of evaluating preclinical therapeutic interventions intended to prevent musculoskeletal deficits after functionally-complete SCI.

Acknowledgements

This work was supported by resources provided by the North Florida/South Georgia Veterans Health System and by work supported by the Office of Research and Development, Rehabilitation Research and Development (RR&D) Service, Department of Veterans Affairs (VA RR&D SPiRE 1I21RX001373-01 and CDA-2 B7733-W) and the National Institutes of Health (P01 HD059751-01A1).

References

1. Giangregorio L, McCartney N. Bone loss and muscle atrophy in spinal cord injury: epidemiology, fracture prediction, and rehabilitation strategies. J Spinal Cord Med 2006;29:489-500.
2. Eser P, Frotzler A, Zehnder Y, Wick L, Knecht H, Denoth J, Schiessl H. Relationship between the duration of paralysis and bone structure: a pQCT study of spinal cord injured individuals. Bone 2004;34:869-80.
3. Frisbie JH. Fractures after myelopathy: the risk quantified. J Spinal Cord Med 1997;20:66-9.
4. Eser P, Frotzler A, Zehnder Y, Denoth J. Fracture threshold in the femur and tibia of people with spinal cord injury as determined by peripheral quantitative computed tomography. Arch Phys Med Rehabil 2005;86:498-504.
5. Morse LR, Battaglino RA, Stolzmann KL, Hallett LD,

Waddimba A, Gagnon D, Lazzari AA, Garshick E. Osteoporotic fractures and hospitalization risk in chronic spinal cord injury. Osteoporos Int 2009;20:385-92.
6. Bryson JE, Gourlay ML. Bisphosphonate use in acute and chronic spinal cord injury: a systematic review. J Spinal Cord Med 2009;32:215-25.
7. Biering-Sorensen F, Hansen B, Lee BS. Non-pharmacological treatment and prevention of bone loss after spinal cord injury: a systematic review. Spinal Cord 2009; 47:508-18.
8. Hartkopp A, Murphy RJ, Mohr T, Kjaer M, Biering-Sorensen F. Bone fracture during electrical stimulation of the quadriceps in a spinal cord injured subject. Arch Phys Med Rehabil 1998;79:1133-6.
9. Giangregorio L, Blimkie CJ. Skeletal adaptations to alterations in weight-bearing activity: a comparison of models of disuse osteoporosis. Sports Med 2002;32:459-76.
10. Sengupta S, Arshad M, Sharma S, Dubey M, Singh MM. Attainment of peak bone mass and bone turnover rate in relation to estrous cycle, pregnancy and lactation in colony-bred Sprague-Dawley rats: suitability for studies on pathophysiology of bone and therapeutic measures for its management. J Steroid Biochem Mol Biol 2005; 94:421-9.
11. Jiang SD, Jiang LS, Dai LY. Changes in bone mass, bone structure, bone biomechanical properties, and bone metabolism after spinal cord injury: a 6-month longitudinal study in growing rats. Calcif Tissue Int 2007;80:167-75.
12. Basso DM, Beattie MS, Bresnahan JC. Graded histological and locomotor outcomes after spinal cord contusion using the NYU weight-drop device versus transection. Exp Neurol 1996;139:244-56.
13. Gregory CM, Vandenborne K, Castro MJ, Dudley GA. Human and rat skeletal muscle adaptations to spinal cord injury. Can J Appl Physiol 2003;28:491-500.
14. Yarrow JF, Conover CF, Beggs LA, Beck DT, Otzel DM, Balaez A, Combs SM, Miller JR, Ye F, Aguirre JI, Neuville KG, Williams AA, Conrad BP, Gregory CM, Wronski TJ, Bose PK, Borst SE. Testosterone dose dependently prevents bone and muscle loss in rodents after spinal cord injury. J Neurotrauma 2014;31:834-45.
15. Liu M, Bose P, Walter GA, Thompson FJ, Vandenborne K. A longitudinal study of skeletal muscle following spinal cord injury and locomotor training. Spinal Cord 2008;46:488-93.
16. Voor MJ, Brown EH, Xu Q, Waddell SW, Burden RL, Jr., Burke DA, Magnuson DS. Bone loss following spinal cord injury in a rat model. J Neurotrauma 2012;29:1676-82.
17. Ye F, Baligand C, Keener JE, Vohra R, Lim W, Ruhella A, Bose P, Daniels M, Walter GA, Thompson F, Vandenborne K. Hindlimb muscle morphology and function in a new atrophy model combining spinal cord injury and cast immobilization. J Neurotrauma 2013;30:227-35.
18. Bose PK, Hou J, Parmer R, Reier PJ, Thompson FJ. Altered patterns of reflex excitability, balance, and locomotion following spinal cord injury and locomotor training. Front Physiol 2012;3:258.
19. Liu M, Bose P, Walter GA, Anderson DK, Thompson FJ, Vandenborne K. Changes in muscle T2 relaxation properties following spinal cord injury and locomotor training. Eur J Appl Physiol 2006;97:355-61.
20. Jayaraman A, Liu M, Ye F, Walter GA, Vandenborne K. Regenerative responses in slow- and fast-twitch muscles following moderate contusion spinal cord injury and locomotor training. Eur J Appl Physiol 2013;113:191-200.
21. Liu M, Stevens-Lapsley JE, Jayaraman A, Ye F, Conover C, Walter GA, Bose P, Thompson FJ, Borst SE, Vandenborne K. Impact of treadmill locomotor training on skeletal muscle IGF1 and myogenic regulatory factors in spinal cord injured rats. Eur J Appl Physiol 2010;109:709-20.
22. Pelker RR, Friedlaender GE, Markham TC, Panjabi MM, Moen CJ. Effects of freezing and freeze-drying on the biomechanical properties of rat bone. J Orthop Res 1984;1:405-11.
23. Chen B, Li Y, Yang X, Xie D. Femoral metaphysis bending test of rat: introduction and validation of a novel biomechanical testing protocol for osteoporosis. J Orthop Sci 2012;17:70-6.
24. Morse L, Teng YD, Pham L, Newton K, Yu D, Liao WL, Kohler T, Muller R, Graves D, Stashenko P, Battaglino R. Spinal cord injury causes rapid osteoclastic resorption and growth plate abnormalities in growing rats (SCI-induced bone loss in growing rats). Osteoporos Int 2008;19:645-52.
25. Morse LR, Lazzari AA, Battaglino R, Stolzmann KL, Matthess KR, Gagnon DR, Davis SA, Garshick E. Dual energy x-ray absorptiometry of the distal femur may be more reliable than the proximal tibia in spinal cord injury. Arch Phys Med Rehabil 2009;90:827-31.
26. Sengupta P. A scientific review of age determination for a laboratory rat: How old is it in comparison with human age? Biomedicine International 2011;2:81-9.
27. Zehnder Y, Luthi M, Michel D, Knecht H, Perrelet R, Neto I, Kraenzlin M, Zach G, Lippuner K. Long-term changes in bone metabolism, bone mineral density, quantitative ultrasound parameters, and fracture incidence after spinal cord injury: a cross-sectional observational study in 100 paraplegic men. Osteoporos Int 2004;15:180-9.
28. Dudley-Javoroski S, Shields RK. Longitudinal changes in femur bone mineral density after spinal cord injury: effects of slice placement and peel method. Osteoporos Int 2010;21:985-95.
29. Frotzler A, Berger M, Knecht H, Eser P. Bone steady-state is established at reduced bone strength after spinal cord injury: a longitudinal study using peripheral quantitative computed tomography (pQCT). Bone 2008;43:549-55.
30. Alexandre C, Vico L. Pathophysiology of bone loss in disuse osteoporosis. Joint Bone Spine 2011;78:572-6.
31. Bloomfield SA. Disuse osteopenia. Curr Osteoporos Rep 2010;8:91-7.
32. Jiang SD, Yang YH, Chen JW, Jiang LS. Isolated osteoblasts from spinal cord-injured rats respond less to me-

chanical loading as compared with those from hindlimb-immobilized rats. J Spinal Cord Med 2013;36:220-4.
33. Zamarioli A, Battaglino RA, Morse LR, Sudhakar S, Maranho DA, Okubo R, Volpon JB, Shimano AC. Standing frame and electrical stimulation therapies partially preserve bone strength in a rodent model of acute spinal cord injury. Am J Phys Med Rehabil 2013;92:402-10.
34. Maraval A, Grados F, Royant V, Damade R, Boulu G, Fardellone P. Longitudinal femoral shaft due to bone insufficiency. A review of three cases. Joint Bone Spine 2003;70:526-31.
35. Williams M, Laredo JD, Setbon S, Belange G, Timsit MA, Karneff A, Pertuiset E. Unusual longitudinal stress fractures of the femoral diaphysis: report of five cases. Skeletal Radiol 1999;28:81-5.
36. Mittra E, Rubin C, Qin YX. Interrelationship of trabecular mechanical and microstructural properties in sheep trabecular bone. J Biomech 2005;38:1229-37.
37. Liu D, Zhao CQ, Li H, Jiang SD, Jiang LS, Dai LY. Effects of spinal cord injury and hindlimb immobilization on sublesional and supralesional bones in young growing rats. Bone 2008;43:119-25.